JOURNAL OF AIRCRAFT
Vol. 47, No. 1, January–February 2010

Free Vibration Analysis of Curvilinear-Stiffened Plates and Experimental Validation

Ali Yeilaghi Tamijani,* Thomas McQuigg,† and Rakesh K. Kapania‡
Virginia Polytechnic Institute and State University, Blacksburg, Virginia 24061

DOI: 10.2514/1.44613

In this research, the vibration analysis of plates with curvilinear stiffeners is carried out. The Ritz method is applied while stiffeners are considered as discrete elements. The first-order shear deformation theory is used to represent the plate and stiffener. Chebyshev polynomial functions are used as the basic functions in the Ritz method. The major part of this work is concerned with modeling the curvilinear stiffeners and comparing the results with experimental data. By considering the curvilinear stiffeners, the curvature, the continuous variation in orientation, can be used in controlling different mode shapes in addition to the associated frequencies. It can provide a mechanism to passively control the dynamic response under certain excitations. In the present method, the geometric properties of curvilinear stiffeners can be modified without changing the plate geometric properties. In the developed formulations, both eccentric and concentric stiffeners were studied. Natural frequencies for plates with straight stiffeners were compared with the results available in the literature. A good agreement was seen. A 24 by 28 in. curvilinear-stiffened panel was machined from 2219-T851 aluminum for experimental validation of the Ritz and meshfree method of vibration mode shape predictions. Results were obtained for this panel mounted vertically to a steel clamping bracket using acoustic excitation and a laser vibrometer. Experimental results appear to correlate well with theoretical predictions.

Nomenclature

A = area
A_b = shear area
a = width of the plate
b = height of the plate
b_s = width of the stiffener
D = flexural rigidity of the plate
$\det J$ = Jacobian of the transformation
E = elastic modulus of the plate
E_s = elastic modulus of the stiffener
G = shear modulus of the plate
G_s = shear modulus of the stiffener
h_p = thickness of the plate
h_s = height of the stiffener
I = second moment of the stiffener cross-sectional area
J_s = torsional stiffness of the stiffener
K_G = shear correction factor of the plate
K_p = plate stiffness matrix
K_s = stiffener stiffness matrix
L = Lagrangian
M_p = plate mass matrix
M_s = stiffener mass matrix
T_p = plate kinetic energy
T_s = stiffener kinetic energy
t = stiffener tangential direction
U_p = plate strain energy
U_s = stiffener strain energy
u_p = plate displacement along the x direction
u_s = stiffener displacement along the t direction
υ = Poisson's ratio
v_p = plate displacement along the y direction
v_s = stiffener displacement along the n direction
w = amplitude of w_p
w_p = plate displacement along the z direction
w_s = stiffener displacement along the b direction
α = the angle between the stiffener tangential direction (t) and the x axis
ζ = natural coordinate
θ_n = stiffener rotation with respect to the t direction
θ_t = stiffener rotation with respect to the n direction
Λ = coordinate transformation matrix
λ = frequency parameter
ϕ_{px} = rotations of normal to the plate midsurface about the y axes
ϕ_{py} = rotations of normal to the plate midsurface about the x axes
φ_x = amplitude of ϕ_x
φ_y = amplitude of ϕ_y
ω = natural frequency
$1/R$ = curvature

I. Introduction

THIS research considers the vibrations of a plate reinforced by a number of curvilinear stiffeners. There are many practical applications of such structures, for example, in aerospace industries, the wings or fuselage of an aircraft; in ship industries, the hull and the deck; and in construction industries, the bridges and offshore structures. Thus, it is not surprising that a considerable number of papers have been devoted to the study of this problem. The plate can be stiffened by curvilinear stiffeners in various ways, by changing the location and the curvature of stiffeners, as well as the dimensions of the stiffeners to achieve better vibration, buckling, and performance under static loads with a relatively lesser amount of material, thus satisfying the objective of minimizing the weight of the structure.

Smith et al. [1] used the Rayleigh–Ritz method, with a polynomial based displacement function, to study the buckling behavior of rectangular plates. They studied different aspect ratios and combinations of clamped, simply supported, and free edges. The simple and classical orthogonal polynomials are used in the Ritz method. The

Presented at the AIAA Region I Young Professional, Student and Education Conference, Baltimore, MD, 21–22 November 2008. Received 28 March 2009; accepted for publication 21 August 2009.

*Ph.D. Candidate, Department of Engineering Science and Mechanics; ayt@vt.edu. Member AIAA.
†Ph.D. Candidate, Department of Aerospace and Ocean Engineering; tmcquigg@vt.edu. Student Member AIAA.
‡Mitchell Professor, Department of Aerospace and Ocean Engineering; rkapania@vt.edu. Associate Fellow AIAA.

orthogonal polynomials were Chebyshev, Hermite, Legendre, and Laguerre. They showed that orthogonal polynomials have better convergence characteristics in plate buckling problems and that the simple polynomial is the preferred displacement function for unilateral plate analysis due to its simplicity and computational speed for iterative solution procedures. Unilateral systems are systems that are restricted to displace or buckle in one direction. The free vibration analysis of intermediate stiffeners [2] and inclined stiffeners [3] was studied by Liew et al. The Mindlin theory was incorporated to derive the formulation; the transverse shear deformation is included in their formulation. Liew et al. [2,3] used the Ritz method with a set of simple polynomials, and their approach was able to enforce the different geometric boundary conditions of various plates considered. A stiffened plate element for the analysis of laminated stiffened plates has been developed by Kumar and Mukhopadhyay [4]. The stiffened plate element includes the effects of transverse shear. The element has no restrictions on the mesh division and can include any number of stiffeners.

The differential quadrature (DQ) method proposed by Bellman et al. [5] has been used in the area of plate analysis and a large number of publications can be found in the literature. Zeng and Bert [6] studied the free vibration of eccentrically stiffened plates by using DQ. The DQ is a numerical technique for initial and boundary value problems. It is based on the approximation of a function and, hence, its partial derivatives with respect to the space variables, within a domain, by a linear sum of function values at all discrete grid points. The discrete singular convolution (DSC) method was developed by Wei et al. [7] and was implemented to analyze the free vibration of a plate. The DSC algorithm is based on the distribution and wavelet theories. Numerical solutions to the differential equations are formulated via the singular kernels of data type. The DSC is able to predict high frequencies of plates (Zhao et al. [8]); however, the versatility and applicability of the DSC method for more complicated structures have not been reported.

The moving least square (MLS) method reconstructs continuous functions from a set of data. Researchers have applied the MLS technique in the analysis of solid mechanics problems by developing the meshfree method (Yeilaghi Tamijani and Kapania [9]). Recently, the MLS data interpolation technique was used to establish the Ritz method for the vibration analysis of plates by Zhou and Zheng [10]. The geometric boundary conditions of the plate can be enforced through a point substitution technique. They studied the convergence, the influence of the MLS mesh size, the MLS support radius, and the number of Gaussian integration points.

In the present study, the Ritz method is employed to analyze the vibration of the plate with curvilinear stiffeners. The energy technique has been used to develop the formulation. The first-order shear deformation theory (FSDT) is used to formulate the kinetic and strain energy of the plate and stiffeners. The Chebyshev polynomial functions are used to parameterize the displacement and rotations. Though vibration analysis of plates with straight stiffeners using the Ritz method with simple polynomials has been already presented [2,3], the vibration analysis of plates with curvilinear stiffeners using Chebyshev polynomials is done by the authors for the first time.

The arbitrary orientation, curvature, location, and eccentricity of the stiffener have been taken into account; however, because in the present study the in-plane deformations were not taken into account, the eccentricity effect on the in-plane deformations was not considered and only the effect on the second moment of the stiffener cross-sectional area was studied. Using the Ritz method gives us the capability to avoid the selection of an appropriate element and the generation of an appropriate mesh, which are needed in the finite element method. Consequently, the stiffeners can be located anywhere in the plate and its geometric properties can be modified without changing the plate properties. The versatility of the developed theory has been applied to various stiffened plates using straight or curvilinear stiffeners.

A single 24 by 28 in. aluminum curvilinear-stiffened plate was designed and experimentally tested to determine natural frequencies and associated mode shapes. The test plate was designed and fabricated in-house. For testing, it was bolted to a solid steel clamp on one end and it was placed vertically in front of a generic public address system speaker that was used for an acoustic excitation. Response was measured using a Polytec laser vibrometer and data were collected from a dSpace analog-to-digital converter board using a MATLAB®-running PC. Results were then analyzed with the help of STAR Modal® [11] software. Frequencies and mode shapes compared well with those obtained using the Ritz method presented here as well as to our earlier meshfree method [9] and seem to verify those results.

II. Mathematical Formulation for Stiffened Plate

In the present formulation, it is assumed that the deformations remain small so that linear relations can be used to represent the strain in the plate and the stiffeners. The emphasis of the present work is on developing a Ritz method based on Chebyshev polynomials for the analysis of an isotropic plate with curvilinear stiffeners. Using the Ritz method and developing the equations for the plate and stiffeners separately will give us the capability to evaluate the mass and stiffness matrices of the stiffener independently of those of the plate.

For simplicity and generality in mathematical formulation, some dimensionless parameters are introduced (Fig. 1):

$$\bar{x} = \frac{x}{a} \qquad \bar{y} = \frac{y}{b} \tag{1}$$

A. Strain and Kinetic Energy of the Plate

Based on FSDT, the transverse displacements and rotations in the plate are assumed in the following form:

$$\begin{aligned} u_p(\bar{x}, \bar{y}, z, t) &= z\phi_x(\bar{x}, \bar{y}, t) \\ v_p(\bar{x}, \bar{y}, z, t) &= z\phi_y(\bar{x}, \bar{y}, t) \\ w_p(\bar{x}, \bar{y}, z, t) &= w_p(\bar{x}, \bar{y}, t) \end{aligned} \tag{2}$$

here ϕ_{px}, and ϕ_{py} are the rotations normal to the midsurface about the y and x axes, respectively, and w_p implies the transverse displacement of a point in the midsurface.

For free vibration of the plate with curvilinear stiffeners, one has

$$\begin{aligned} \phi_x(\bar{x}, \bar{y}, t) &= \varphi_x(\bar{x}, \bar{y})e^{i\omega t} \\ \phi_y(\bar{x}, \bar{y}, t) &= \varphi_y(\bar{x}, \bar{y})e^{i\omega t} \\ w_p(\bar{x}, \bar{y}, t) &= w(\bar{x}, \bar{y})e^{i\omega t} \end{aligned} \tag{3}$$

where $\varphi_x(\bar{x}, \bar{y})$, $\varphi_y(\bar{x}, \bar{y})$, and $w(\bar{x}, \bar{y})$ are the amplitude of $\phi_x(\bar{x}, \bar{y}, t)$, $\phi_y(\bar{x}, \bar{y}, t)$, and $w_p(\bar{x}, \bar{y}, t)$, respectively. Also, ω is the natural frequency of the structure. From the displacement field, defined in Eq. (2), the strain components are defined as

$$\varepsilon_p = \begin{Bmatrix} \gamma_{pxz} \\ \gamma_{pyz} \\ \kappa_{px} \\ \kappa_{py} \\ \kappa_{pxy} \end{Bmatrix} = \begin{bmatrix} 1 & 0 & \frac{1}{a}\frac{\partial}{\partial \bar{x}} \\ 0 & 1 & \frac{1}{b}\frac{\partial}{\partial \bar{y}} \\ \frac{1}{a}\frac{\partial}{\partial \bar{x}} & 0 & 0 \\ 0 & \frac{1}{b}\frac{\partial}{\partial \bar{y}} & 0 \\ \frac{1}{b}\frac{\partial}{\partial \bar{y}} & \frac{1}{a}\frac{\partial}{\partial \bar{x}} & 0 \end{bmatrix} \begin{Bmatrix} \varphi_x \\ \varphi_y \\ w \end{Bmatrix} \tag{4}$$

The strain and kinetic energies of the plate, respectively, can be expressed as [3]

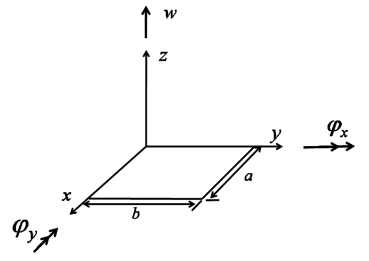

Fig. 1 Directions of the generalized displacements of the plate.

$$U_p = \frac{1}{2}\int_0^1\int_0^1\left[D\left(\left(\frac{1}{a}\frac{\partial\varphi_x}{\partial\bar{x}}\right)^2 + \left(\frac{1}{b}\frac{\partial\varphi_y}{\partial\bar{y}}\right)^2 + 2\upsilon\left(\frac{1}{ab}\frac{\partial\varphi_x}{\partial\bar{x}}\frac{\partial\varphi_y}{\partial\bar{y}}\right) + \frac{1-\upsilon}{2}\left(\frac{1}{b}\frac{\partial\varphi_x}{\partial\bar{y}} + \frac{1}{a}\frac{\partial\varphi_y}{\partial\bar{x}}\right)^2\right) + K_G G h_p\left(\left(\varphi_x + \frac{1}{a}\frac{\partial w}{\partial\bar{x}}\right)^2 + \left(\varphi_y + \frac{1}{b}\frac{\partial w}{\partial\bar{y}}\right)^2\right)\right] ab\,\mathrm{d}\bar{x}\,\mathrm{d}\bar{y}$$

$$T_p = \frac{1}{2}\rho\omega^2\int_0^1\int_0^1\left[h_p w^2 + \frac{1}{12}h_p^3(\varphi_x^2 + \varphi_y^2)\right] ab\,\mathrm{d}\bar{x}\,\mathrm{d}\bar{y} \tag{5}$$

where D, K_G, G, E, h_p, a, and b are the flexural rigidity, shear correction factor, shear modulus, elastic modulus, thickness, width, and height of the plate, respectively.

B. Strain and Kinetic Energy of the Stiffener

The arbitrary shape of the curvilinear stiffener is mapped to a region [0, 1] in the ζ coordinate (Fig. 2c) with the help of η_i shape functions [12]:

$$\bar{x} = \sum_{i=1}^{np}\eta_i(\zeta)\bar{x}_i \qquad \bar{y} = \sum_{i=1}^{np}\eta_i(\zeta)\bar{y}_i \tag{6}$$

where $(\bar{x}_i, \bar{y}_i)$ are the coordinates of the ith point on the curvilinear stiffener in the $\bar{x}$–$\bar{y}$ plane, np is the number of points, and ζ is the natural coordinate for parameterization of the curve (Fig. 2c). The stiffener strain vector is [12]

$$\begin{cases} \gamma_n = \frac{\mathrm{d}w_s}{\mathrm{d}s} + \theta_t \\ \kappa_t = \frac{\mathrm{d}\theta_t}{\mathrm{d}s} + \frac{\theta_n}{R} \\ \kappa_n = \frac{\mathrm{d}\theta_n}{\mathrm{d}s} - \frac{\theta_t}{R} \end{cases} \qquad \begin{aligned} s(\zeta) &= \textstyle\int_0^\zeta \det J\,\mathrm{d}\zeta \\ \det J &= \sqrt{\left(a\frac{\mathrm{d}\bar{x}}{\mathrm{d}\zeta}\right)^2 + \left(b\frac{\mathrm{d}\bar{y}}{\mathrm{d}\zeta}\right)^2} \end{aligned} \tag{7}$$

where $\det J$ is the Jacobian of the transformation and R is the radius of curvature [9] (Fig. 2a). θ_t, θ_n, and w_s, which are the rotations about the normal (n) and tangential (t) directions, respectively, and the deflection along the binormal direction (b), are shown in Fig. 2b. Using Eq. (6), the rotations and deflection can be expressed as

$$\begin{cases} \theta_t = \theta_t(\bar{x}(\zeta), \bar{y}(\zeta)) \\ \theta_n = \theta_n(\bar{x}(\zeta), \bar{y}(\zeta)) \\ w_s = w_s(\bar{x}(\zeta), \bar{y}(\zeta)) \end{cases} \tag{8}$$

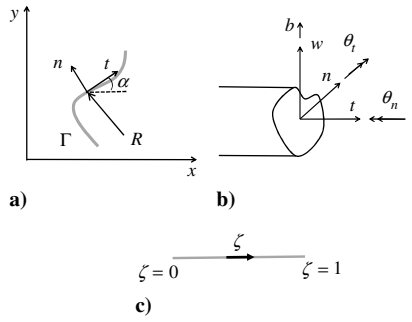

Fig. 2 Curvilinear stiffener: a) local and global coordinate systems, b) directions of the generalized displacements, and c) the transformed plane.

The strain and kinetic energy of the stiffener can be defined as [9]

$$U_s = \frac{1}{2}\int_\Gamma\left[G_s A_b\left(\theta_t + \frac{\mathrm{d}w_s}{\mathrm{d}s}\right)^2 + G_s J_s\left(\frac{\mathrm{d}\theta_n}{\mathrm{d}s} - \frac{\theta_t}{R}\right)^2 + E_s I_n\left(\frac{\mathrm{d}\theta_t}{\mathrm{d}s} + \frac{\theta_n}{R}\right)^2\right]\mathrm{d}s$$

$$T_s = \frac{1}{2}\rho_s\omega^2\int_\Gamma[A w_s^2 + I_n\theta_t^2 + (I_n + I_t)\theta_n^2]\,\mathrm{d}s \tag{9}$$

where A_b, A, I, J_s, G_s, and E_s are the shear area, area, second moment of the stiffener cross-sectional area about the reference axis, torsional stiffness of the stiffener (using St. Venant's torsion constant), shear modulus, and elastic modulus of the stiffener, respectively.

As a general case, a curved stiffener having eccentricity with respect to the midplane of the plate, and placed anywhere on the plate, is considered as shown in Fig. 2a. Because the stiffener is a curved one, its direction changes from point to point; hence, a local axis (t) is considered along the tangent to the stiffener at the Gaussian integration point, making an angle α with the global axis (x) (Fig. 2a), which is defined by

$$u_s' = \begin{Bmatrix} \theta_t \\ \theta_n \\ w_s \end{Bmatrix} = \begin{bmatrix} \cos\alpha & \sin\alpha & 0 \\ -\sin\alpha & \cos\alpha & 0 \\ 0 & 0 & 1 \end{bmatrix}\begin{Bmatrix} \varphi_x \\ \varphi_y \\ w \end{Bmatrix} = \Lambda u_s \tag{10}$$

where Λ is the coordinate transformation matrix.

C. Parameterization of Deflections and Rotations

It is known that a choice of admissible functions is very important to the accuracy and efficiency of the solutions obtained by the Ritz method; there are several types of functions, such as beam characteristic functions, simple polynomials, and orthogonal characteristic polynomials, which were employed when dealing with free vibration problems successfully [13–15]. In this research, a set of Chebyshev polynomials is selected for the Ritz method. Each of the displacement and rotations functions can be written as double series of Chebyshev polynomials multiplied by boundary functions:

$$\begin{cases} \varphi_x(\bar{x},\bar{y}) = \sum_{m=1}^{p_1}\sum_{n=1}^{q_1} c_{mn}\psi_{xmn}(\bar{x},\bar{y}) \\ \varphi_y(\bar{x},\bar{y}) = \sum_{m=1}^{p_2}\sum_{n=1}^{q_2} d_{mn}\psi_{ymn}(\bar{x},\bar{y}) \\ w(\bar{x},\bar{y}) = \sum_{m=1}^{p_3}\sum_{n=1}^{q_3} e_{mn}\varphi_{mn}(\bar{x},\bar{y}) \end{cases} \qquad \begin{cases} \psi_{xmn}(\bar{x},\bar{y}) = \psi_{bx}(\bar{x},\bar{y})X_m(\bar{x})Y_n(\bar{y}) \\ \psi_{ymn}(\bar{x},\bar{y}) = \psi_{by}(\bar{x},\bar{y})X_m(\bar{x})Y_n(\bar{y}) \\ \varphi_{mn}(\bar{x},\bar{y}) = \varphi_b(\bar{x},\bar{y})X_m(\bar{x})Y_n(\bar{y}) \end{cases} \tag{11}$$

where c_{mn}, d_{mn}, and e_{mn} are the unknown coefficients and p_s and q_s ($s = 1, 2$, and 3) are the degrees of the Chebyshev polynomials in the $\bar{x}$ and $\bar{y}$ directions, respectively. $X_m(\bar{x})$ and $Y_n(\bar{y})$ are one-dimensional Chebyshev polynomials $P_i(\chi)$:

$$P_i(\chi) = \cos[(i-1)\arccos(\chi)], \quad i = 1, 2, \ldots; \quad \chi = \bar{x}, \bar{y} \tag{12}$$

Also, $\psi_{bx}(\bar{x},\bar{y})$, $\psi_{by}(\bar{x},\bar{y})$, and $\varphi_b(\bar{x},\bar{y})$ are polynomial expressions describing the boundary conditions that are functions of the plate geometry and kinematics. The nondimensionalized boundary polynomial expressions for a rectangular plate with varying boundary conditions are [2]

$$\psi_{bx}(\bar{x},\bar{y}), \qquad \psi_{by}(\bar{x},\bar{y}) \quad \text{and} \quad \varphi_b(\bar{x},\bar{y}) = \prod_{j=1}^{4}[\Gamma_j(\bar{x},\bar{y})]^{\Omega_j} \tag{13}$$

where Γ_j is the boundary equation of the jth supporting edge and Ω_j, depending on the support edge condition, is shown in Table 1.

Table 1 Plate boundary equations

	φ_x	φ_y	w
$\Omega_j = 0$	If the jth edge is free or simply supported in the y direction	If the jth edge is free or simply supported in the x direction	If the jth edge is free
$\Omega_j = 1$	If the jth edge is clamped or simply supported in the x direction	If the jth edge is clamped or simply supported in the y direction	If the jth edge is clamped or simply supported

D. Natural Frequencies and Mode Shapes of the Plate with Curvilinear Stiffener

The Lagrangian L of the stiffened plate is defined as

$$L = T_p + T_s - U_p - U_s \tag{14}$$

By substituting Eq. (11) in Eq. (5),

$$\begin{cases} U_p = \frac{1}{2} C^T \int_0^1 \int_0^1 B_p^T D_p B_p ab \, \mathrm{d}\bar{x} \, \mathrm{d}\bar{y} \, C \\ T_p = \frac{1}{2} \omega^2 C^T \int_0^1 \int_0^1 N_p^T m_p N_p ab \, \mathrm{d}\bar{x} \, \mathrm{d}\bar{y} \, C \end{cases}, \quad C = \begin{Bmatrix} \boldsymbol{c} \\ \boldsymbol{d} \\ \boldsymbol{e} \end{Bmatrix} \tag{15}$$

where B_p, N_p, D_p, and m_p are defined in the Appendix. By using Eqs. (10) and (11), Eq. (9) can be written as

$$\begin{cases} U_s = \frac{1}{2} C^T \int_0^1 B_s^T D_s B_s \det J \, \mathrm{d}\zeta C \\ T_s = \frac{1}{2} \omega^2 C^T \int_0^1 N_s^T m_s N_s \det J \, \mathrm{d}\zeta C \end{cases} \tag{16}$$

where B_s, N_s, D_s, and m_s are given in the Appendix.

Minimization of the maximum strain and kinetic energies of the stiffened plate with respect to the c_{mn}, d_{mn}, and e_{mn} leads to a set of linear eigenvalue equations [2,3]:

$$((K_p + K_s) - \omega^2 (M_p + M_s))C = 0 \tag{17}$$

where the plate and stiffener stiffness (K_p and K_s) and mass (M_p and M_s) matrices are defined in the Appendix. Equation (17) is the characteristic equation of the stiffened plate.

III. Convergence and Comparison Studies

As is known, the Ritz method can provide accurate solutions. However, its convergence depends on the choice of global admissible functions. The natural frequencies obtained by the Ritz method converge as upper bounds to the exact values. These upper bound estimates could be improved by increasing the number of terms in functions. Using different kinds of functions can increase or decrease the number of terms for which the results converge. To illustrate the versatility of the current method, numerical examples have been performed by using MATLAB. To decide upon the number of terms to be used in the assumed expansion, the convergence of the solutions with increasing numbers of terms being used in the assumed approximations was examined for the natural frequency parameters of the stiffened plate. As expected, it is seen that the convergence using the present approximate method is monotonic. The results are provided for the plate with straight and curvilinear stiffeners with different boundary conditions. The validity of the formulation is shown by comparing the results with the available results in the literature.

A. Plate with a Single Stiffener

The problem selected as the first example to validate the present method is a square plate with a centrally placed stiffener as shown in Fig. 3. Both plate and stiffener are made of the same isotropic material with $\nu = 0.3$. This problem is previously reported by Liew et al. [2]. They studied the application of the Ritz method for this problem by using simple polynomials. The results presented by Liew et al. were obtained for the eccentric stiffener. To make a comparison, this problem was analyzed for an eccentric stiffener using Chebyshev polynomials. The frequency parameter is defined as

$$\lambda = (\omega b^2/\pi^2)\sqrt{\rho h_p/D} \tag{18}$$

In this example, the plate with $a/b = 1$, $h_p/b = 0.05$, $b_s/b = 0.05$, and $h_s/h_p = 1.5$ is considered. The results for the plate that is simply supported and clamped on all edges, as shown in Table 2, show that acceptable convergence has been achieved for the first six frequencies. Also, the results are in good agreement with the previously published results. The convergence of all six natural frequencies in Table 2 indicates the suitability of the Chebyshev polynomials as the basis functions in the Ritz analysis of the stiffened plate.

B. Plate with Two Stiffeners

As shown in Fig. 4, a plate, simply supported on all edges, with cross stiffeners is considered. The natural frequencies are compared with those of Liew et al. [3]. They developed the Ritz method by using simple polynomials based on the Mindlin–Engesser model. The convergence of the first six frequency parameters for the plates with different a/b and h_p/b ratios are presented in Table 3. In Table 3, it can be seen that the solutions generated in both studies are in close agreement. The same convergence trend as shown in Table 2 has been observed when more stiffeners are used in the computation.

C. Plate with Multiple Stiffeners

The plate with multiple stiffeners, simply supported on all edges, is analyzed for free vibrations (see Fig. 5). The convergence and comparison study with different values of the plate aspect ratios a/b and h_p/b are tabulated in Table 4. The natural frequencies, as expected, converge from above and reach acceptable upper bound values. As noted from Tables 2–4, the convergence of the orthogonal polynomials is superior to that of the simple polynomials. The procedure presented here can be used to generate very accurate results for the natural frequencies of rectangular plates with various types of boundary conditions and curvilinear stiffeners.

IV. Experimental Design

Experimental work was used to validate the ability of the Ritz and meshfree [9] methods to realistically predict natural frequencies and mode shapes of curvilinear-stiffened plates. A design for a 24 by 28 in. plate with two curvilinear stiffeners was chosen. For testing, the plate was bolted to a steel bracket to create a clamped condition on one end, while the remaining edges were allowed to remain free. The Virginia Polytechnic Institute and State University Department of Aerospace and Ocean Engineering (AOE) Structures and Engineering Laboratory's single-point Polytec laser vibrometer was used to sense vibration response of the plate to acoustic excitation.

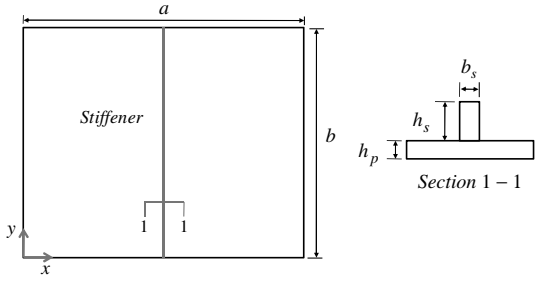

Fig. 3 Plate with central stiffener.

Table 2 Frequency parameters for a square plate with a central stiffener

Clamped plate (CCCC)								
	Simple polynomials (Liew et al. [2])				Chebyshev polynomials			
Mode	10[a]	12	13	14	10	12	13	14
1	4.674	4.654	4.640	4.639	4.643	4.629	4.629	4.616
2	7.139	7.138	7.138	7.138	7.025	7.025	7.025	7.025
3	9.758	9.678	9.669	9.628	9.640	9.594	9.594	9.555
4	10.401	10.399	10.398	10.398	10.258	10.258	10.258	10.258
5	11.967	11.964	11.960	11.960	11.947	11.943	11.943	11.940
6	15.422	15.417	15.416	15.414	15.240	15.239	15.239	15.239
Simply supported plate (SSSS)								
	Simple polynomials (Liew et al. [2])				Chebyshev polynomials			
Mode	10	12	13	14	10	12	13	14
1	2.391	2.389	2.388	2.388	2.384	2.383	2.383	2.381
2	4.948	4.948	4.948	4.948	4.897	4.897	4.897	4.897
3	6.851	6.822	6.822	6.801	6.798	6.775	6.773	6.757
4	7.866	7.865	7.864	7.864	7.791	7.791	7.791	7.791
5	9.107	9.105	9.104	9.104	9.091	9.089	9.089	9.088
6	12.482	12.397	12.334	12.333	12.312	12.263	12.257	12.229

[a]Degree of polynomial considered in the expansion.

Table 3 Frequency parameters for a rectangular plate with cross stiffeners

$a/b = 1$		$h_p/b = 0.05$			$b_s/b = 0.01$		$h_s/h_p = 1.5$	
	Simple polynomials (Liew et al. [3])				Chebyshev polynomials			
Mode	10[a]	12	13	14	10	12	13	14
1	2.463	2.460	2.458	2.458	2.456	2.452	2.450	2.450
2	5.915	5.907	5.906	5.896	5.890	5.878	5.875	5.868
3	5.916	5.908	5.908	5.897	5.890	5.878	5.875	5.868
4	9.323	9.290	9.256	9.255	9.241	9.199	9.187	9.167
5	10.213	10.201	10.194	10.193	10.194	10.182	10.177	10.175
6	11.930	11.870	11.840	11.840	11.833	11.780	11.753	11.740
$a/b = 2$		$h_p/b = 0.001$			$b_s/b = 0.01$		$h_s/h_p = 1.5$	
	Simple polynomials (Liew et al. [3])				Chebyshev polynomials			
Mode	10	12	13	14	10	12	13	14
1	1.463	1.461	1.459	1.459	1.458	1.456	1.455	1.455
2	2.563	2.558	2.558	2.557	2.555	2.552	2.551	2.550
3	4.322	4.309	4.302	4.302	4.296	4.287	4.282	4.282
4	4.930	4.922	4.922	4.906	4.909	4.895	4.890	4.886
5	5.903	5.877	5.850	5.850	5.843	5.814	5.814	5.796
6	6.582	6.543	6.543	6.524	6.523	6.498	6.494	6.483

[a]Degree of polynomial considered in the expansion.

MATLAB and STAR Modal [11] were used for data collection and data analysis, respectively.

A. Experiment Models and Equipment

A 24 by 28 in. curvilinear-stiffened plate was fabricated from 2219–T851 aluminum in the AOE Machine Shop. The geometric and material properties [16] of the plate are shown in Fig. 6. The plate had a thickness of near a quarter of an inch and identically shaped curvilinear stiffeners, each about $1/2$ in. tall and $1/8$ in. inch wide. The plate was clamped at one end during testing to a steel bracket bolted to a heavy steel frame table. Notches at either end of this boundary condition were designed to mechanically separate the main plate from the clamped extra material. Also, the stiffeners of this plate were shortened by approximately $1/2$ in. on either end and beveled at either end at an angle of 30 deg.

Electronic interfaces were handled with a dSpace PPC Controller Board. An analog signal was sent from a PC through a generic Crown signal amplifier to a Cerwin–Vega! 3-in-1 public address speaker which was used for excitation. Single-point measurements were taken by a Polytec OFV-505 Laser Vibrometer, which was positioned using Newport linear motion stages. The analog signal from the Vibrometer was sent through a Multimetrics, Inc., AF-4201 high-pass filter before being converted to a digital signal and stored in the same PC mentioned earlier. Through MATLAB and dSpace Control Desk, the experiment was controlled, including signal creation, stage

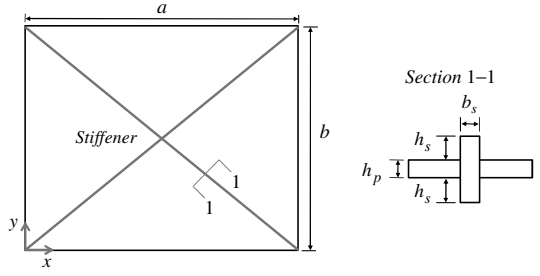

Fig. 4 Plate with cross stiffeners.

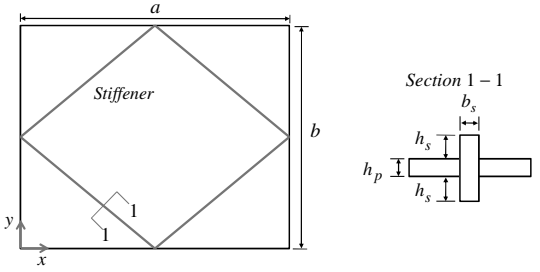

Fig. 5 Plate with multiple stiffeners.

Table 4 Frequency parameters for a rectangular plate with multiple stiffeners

$a/b = 1$		$h_p/b = 0.05$			$b_s/b = 0.01$		$h_s/h_p = 1.5$	
	Simple polynomials (Liew et al. [3])				Chebyshev polynomials			
Mode	10[a]	12	13	14	10	12	13	14
1	2.545	2.542	2.540	2.540	2.539	2.537	2.536	2.535
2	5.923	5.909	5.909	5.903	5.900	5.888	5.884	5.878
3	5.924	5.910	5.910	5.904	5.900	5.888	5.884	5.878
4	9.327	9.289	9.273	9.273	9.257	9.217	9.204	9.186
5	9.777	9.771	9.763	9.763	9.767	9.758	9.754	9.752
6	12.370	12.320	12.280	12.280	12.293	12.230	12.204	12.192
$a/b = 2$		$h_s/b = 0.001$			$b_s/b = 0.01$		$h_s/h_p = 1.5$	
	Simple polynomials (Liew et al. [3])				Chebyshev polynomials			
Mode	10	12	13	14	10	12	13	14
1	1.521	1.519	1.518	1.518	1.518	1.517	1.516	1.516
2	2.563	2.561	2.561	2.558	2.558	2.555	2.554	2.552
3	4.143	4.136	4.131	4.131	4.139	4.128	4.123	4.123
4	4.909	4.918	4.918	4.909	4.915	4.900	4.895	4.889
5	5.910	5.877	5.860	5.860	5.856	5.827	5.827	5.808
6	6.572	6.531	6.531	6.521	6.536	6.498	6.493	6.482

[a]Degree of polynomial considered in the expansion.

motion and positioning, data collection, preprocessing, and storage. The lab setup can be seen in Fig. 7. The experimental procedure is detailed in Sec. IV.B.

B. Experimental Procedure

A MATLAB graphical user interface was created to automate the experiment and control each of the components linked through the dSpace control board. A 24 by 24 point square grid with 1 in. spacing was used to locate the laser at each measurement point. The 23 by 23 in. measured area of the plate was determined by the limitations of the linear motion stages. Once the vibrometer was positioned, the plate was excited by three sign pulse waves in the range of 0–300 Hz. The recorded response for each of the five excitation iterations was averaged. The frequency response function (FRF) was calculated from the averaged response information for each point and stored in local memory until all measurements were complete. After all the measurements were taken at all 576 points, they were written in universal file format (UFF) and saved to the hard drive of the PC.

Following the initial measurements, experimentation was completed by postanalysis done with STAR Modal software. A model was created to mimic the grid of measurement points discussed earlier. Once the correct relationships between the measurement points was established, the UFF file containing the FRF was loaded and assigned to the model. With this information, STAR graphically constructs the plate vibration shape at each frequency within the measurement spectrum. Use of curve fitting is necessary to identify the frequencies of the modal peaks in the FRF. These frequencies and the corresponding mode shapes are the experimental natural frequencies and mode shapes of vibration and are presented in Sec. IV.C.

Fig. 7 Laser vibrometer and support equipment in place for testing.

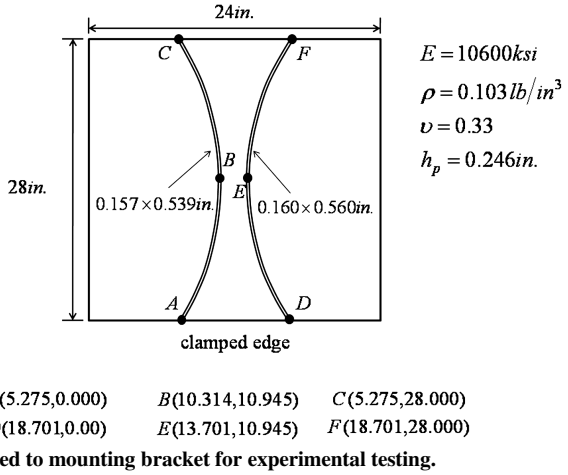

Fig. 6 Curvilinear-stiffened plate bolted to mounting bracket for experimental testing.

C. Results and Discussion

The analytic predictions and experimental results for the vibration mode shapes and frequencies of the curvilinear-stiffened plate are presented in Fig. 8. In the Ritz method, Chebyshev polynomials up to the fourteenth order are used and, in the meshfree code [9], 22×22 particles and 60 particles are considered for the plate and stiffeners, respectively. The mode shapes in Fig. 8 are ordered numerically with respect to the corresponding frequency in hertz. All of the mode shapes are presented with the clamped side at the bottom of the curvilinear-stiffened rectangle. Although the experimental plate was 24 by 28 in. and the analytic plates were also dimensioned to represent the same area, only a 23 by 23 in. area was picked to represent each mode shape in Fig. 8. This is to represent the 23 by 23 in. area that was measured experimentally. A reduced area was

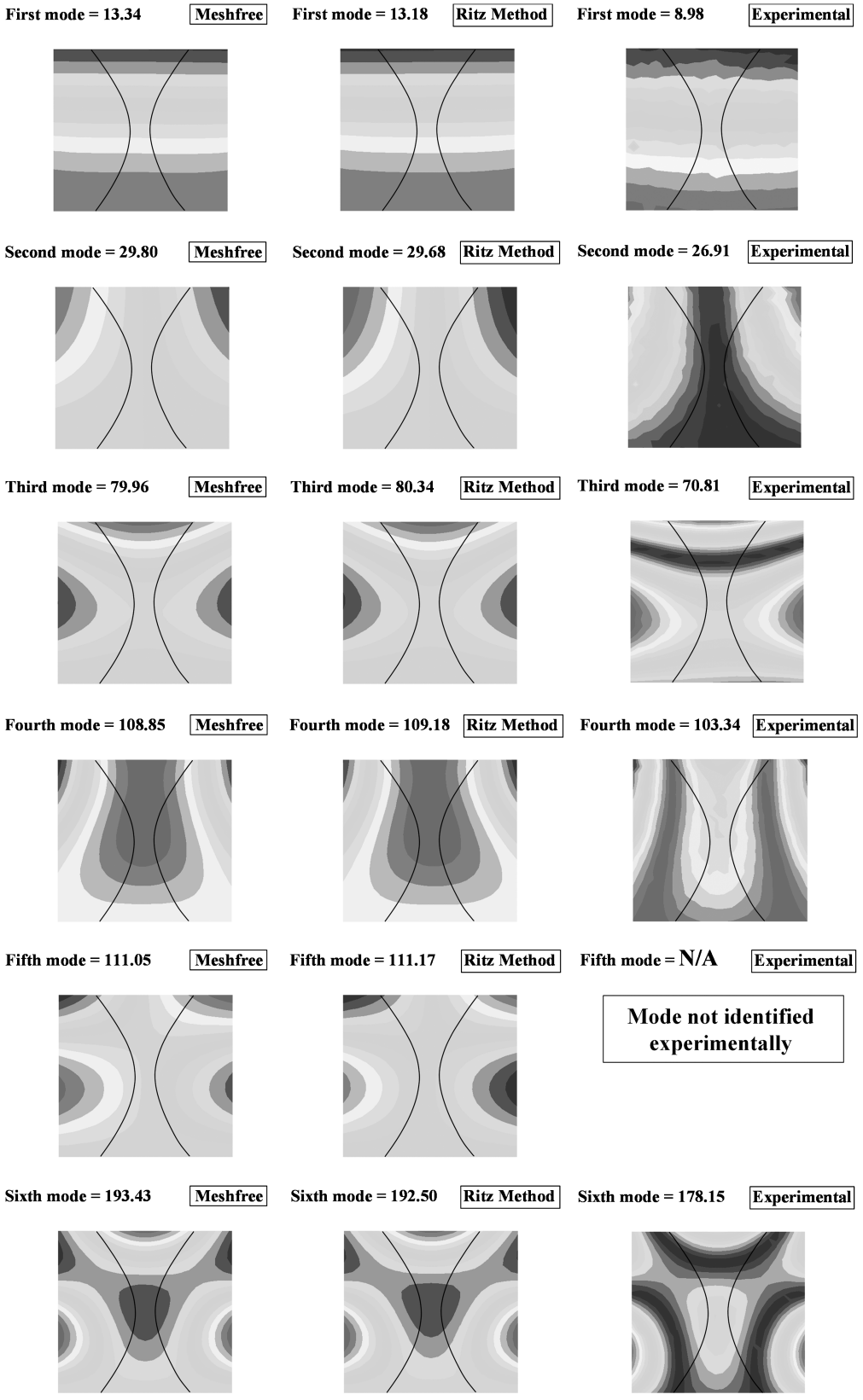

Fig. 8 Comparison of analytic and experimental mode shapes.

measured from the full plate size due to movement limitations of the linear actuation stages. Rather than reposition the stages and overlay the results, a 23 by 23 in. area was picked in the center of the plate to represent the plate response. From the results, this area appears to be sufficient. Overall, the mode shapes correspond well with the appropriate Ritz and meshfree predictions with a few discrepancies.

It can be noted that the analytical frequencies were consistently predicted to be higher than the experimental results shown. The discrepancy varied between 5 and 12% for all of the experimental modes that were successfully documented from the experimental results. The lone mode shape that was not predicted with error in this range was the fundamental. The larger error present in the analytic prediction of this mode can be attributed its location below the lower limit of the operating range of the speaker used for excitation, which was 25 Hz. Also, because this discrepancy is fairly uniform, perhaps an estimation method for reducing this error or the cause could be found and removed, although that cause is unknown at this time.

It is also of interest to compare the CPU time of the Ritz and meshfree methods. The algorithms for both methods are coded in MATLAB and run on a same computer, and it is found that the meshfree code is 15% more efficient in terms of CPU time than the Ritz code. However, it should be noted that the Ritz method code is simpler, more understandable, and easier to debug than the meshfree code.

The fifth mode is indeed missing from the experimental results. Noting that the frequency difference between the fourth and fifth modes is less than 1%, a likely cause is that the amplitude of the fourth mode response is higher in magnitude. For the precision that these measurements were taken with, the fourth mode response may mask the fifth mode.

Some other discrepancies in the results are as follows. The experimentally found second mode has the same general shape as the two analytic predictions, but the resulting shape is symmetric rather than asymmetric with respect to the free corners. A similar pattern is seen in the third mode, in which the free side displacements in the experimental results are all in the same direction, whereas the analytic mode shapes feature opposite displacement directions on the vertical free sides than the horizontal free side. Also, in the fifth mode, the maximum displacement region in the center is split into a U-shaped region by a medium amplitude region. Finally, this same phenomenon is present in the sixth mode.

It is believed that any other imperfections or asymmetries are present only due to material and plate imperfections inherent in any real plate. Furthermore, the boundary conditions at the clamped edge may not be perfectly clamped. This can explain a lower value of the natural frequencies obtained in the experimental results. Overall, the experimental predictions appear to correlate well with the meshfree and Ritz analytic predictions for a plate with curvilinear stiffeners.

V. Conclusions

The paper presents the formulation of a plate with curvilinear stiffeners using the Ritz method based on first-order shear deformation theory. The Chebyshev polynomials are used in the Ritz method. Because the stiffness and mass matrices of the stiffened plate are obtained by superimposing the stiffness and mass matrices of the plate and stiffeners, for modifying the stiffener geometry the plate geometry does not need to be changed. The boundary conditions are imposed by using a set of polynomials that gives us the capability to impose different kinds of boundary conditions. The developed formulation can be applied to arbitrary curvilinear stiffeners. The accuracy of the present formulation was verified through several comparisons with other results available in the literature. The numerical examples indicate that using Chebyshev polynomials up to the fourteenth order as the basis functions in the Ritz method can estimate the first six natural frequencies with a good convergence.

From the experimental studies, the following conclusions can be made. A 23 by 23 in. experimentally measured area of a 24 by 28 in. curvilinear-stiffened plate seems to validate the analytical predictions accomplished using the Ritz and meshfree methods. Overall, the frequencies are overpredicted, but in a seemingly consistent manner (experimental results are lower than the analytical results) that would suggest a relationship (e.g., the clamped edge not being perfectly clamped) could be established for the difference between the analytic and experimental frequencies. The fifth mode was not found experimentally, most likely due to its proximity to the stronger fourth mode. Other discrepancies were either minor shape or symmetry differences. Overall the experiment results seem to correspond well to the predictions, both in terms of mode shape and placement in the frequency domain.

Appendix: Matrices for Chebyshev–Ritz Formulation

The plate flexural rigidity and mass matrices are

$$D_p = \frac{Eh_p}{1-\upsilon^2}\begin{bmatrix} \frac{h_p^2}{12} & & & & \\ \frac{\upsilon h_p^2}{12} & \frac{h_p^2}{12} & & \text{sym.} & \\ 0 & 0 & \frac{h_p^2(1-\upsilon)}{24} & & \\ 0 & 0 & 0 & K_G\frac{1-\upsilon}{2} & \\ 0 & 0 & 0 & 0 & K_G\frac{1-\upsilon}{2} \end{bmatrix}$$

$$m_p = \rho\begin{bmatrix} \frac{1}{12}h_p^3 & & \text{sym.} \\ 0 & \frac{1}{12}h_p^3 & \\ 0 & 0 & h_p \end{bmatrix} \tag{A1}$$

Matrices B_p and N_p, needed for defining the plate strain and displacements vectors, in terms of unknown vector, are

$$[B_p]_{mn}^T = \begin{bmatrix} \frac{1}{a}\frac{\partial\psi_{xmn}}{\partial\bar{x}} & 0 & \frac{1}{b}\frac{\partial\psi_{xmn}}{\partial\bar{y}} & \psi_{xmn} & 0 \\ 0 & \frac{1}{b}\frac{\partial\psi_{ymn}}{\partial\bar{y}} & \frac{1}{a}\frac{\partial\psi_{ymn}}{\partial\bar{x}} & 0 & \psi_{ymn} \\ 0 & 0 & 0 & \frac{1}{a}\frac{\partial\varphi_{mn}}{\partial\bar{x}} & \frac{1}{b}\frac{\partial\varphi_{mn}}{\partial\bar{y}} \end{bmatrix}$$

$$[N_p]_{mn} = \begin{bmatrix} \psi_{xmn} & & \text{sym.} \\ 0 & \psi_{ymn} & \\ 0 & 0 & \varphi_{mn} \end{bmatrix} \tag{A2}$$

The stiffener flexural rigidity and mass matrices are

$$D_s = \begin{bmatrix} EI & & \text{sym.} \\ 0 & GJ & \\ 0 & 0 & GA_b \end{bmatrix}, \quad m_s = \rho_s\begin{bmatrix} I_n & & \text{sym.} \\ 0 & I_t + I_n & \\ 0 & 0 & A \end{bmatrix} \tag{A3}$$

Matrices B_s and N_s for defining the stiffener strain and displacements vectors, in terms of unknown vector, are

$$[N_s]_{mn} = \begin{bmatrix} \psi_{xmn}\cos\alpha & \psi_{ymn}\sin\alpha & 0 \\ -\psi_{xmn}\sin\alpha & \psi_{ymn}\cos\alpha & 0 \\ 0 & 0 & \varphi_{mn} \end{bmatrix}$$

$$[B_s]_{mn} = \begin{bmatrix} B_{11mn} & B_{12mn} & 0 \\ B_{21mn} & B_{22mn} & 0 \\ B_{31mn} & B_{32mn} & B_{33mn} \end{bmatrix}$$

$$\begin{cases} B_{11mn} = \frac{1}{a}\frac{\partial\psi_{xmn}}{\partial\bar{x}}\cos\alpha^2 + \frac{1}{b}\frac{\partial\psi_{xmn}}{\partial\bar{y}}\cos\alpha\sin\alpha - \frac{\sin\alpha}{R}\psi_{xmn} \\ B_{12mn} = \frac{1}{a}\frac{\partial\psi_{ymn}}{\partial\bar{x}}\sin\alpha\cos\alpha + \frac{1}{b}\frac{\partial\psi_{ymn}}{\partial\bar{y}}\sin\alpha^2 + \frac{\cos\alpha}{R}\psi_{ymn} \\ B_{21mn} = -\frac{1}{a}\frac{\partial\psi_{xmn}}{\partial\bar{x}}\sin\alpha\cos\alpha - \frac{1}{b}\frac{\partial\psi_{xmn}}{\partial\bar{y}}\sin\alpha^2 - \frac{\cos\alpha}{R}\psi_{xmn} \\ B_{22mn} = \frac{1}{a}\frac{\partial\psi_{ymn}}{\partial\bar{x}}\cos\alpha^2 + \frac{1}{b}\frac{\partial\psi_{ymn}}{\partial\bar{y}}\cos\alpha\sin\alpha - \frac{\sin\alpha}{R}\psi_{ymn} \\ B_{31mn} = \psi_{xmn}\cos\alpha \qquad B_{32i} = \psi_{ymn}\sin\alpha \\ B_{33mn} = \frac{1}{a}\frac{\partial\varphi_{mn}}{\partial\bar{x}}\cos\alpha + \frac{1}{b}\frac{\partial\varphi_{mn}}{\partial\bar{y}}\sin\alpha \end{cases} \tag{A4}$$

The stiffness and mass matrices for plate and stiffener are given as

$$K_p = \int_0^1 \int_0^1 B_p^T D_p B_p ab \, \mathrm{d}\bar{x} \, \mathrm{d}\bar{y}$$

$$M_p = \int_0^1 \int_0^1 N_p^T m_p N_p ab \, \mathrm{d}\bar{x} \, \mathrm{d}\bar{y}$$

$$K_s = \int_0^1 B_s^T D_s B_s \det J \, \mathrm{d}\zeta$$

$$M_s = \int_0^1 N_s^T m_s N_s \det J \, \mathrm{d}\zeta \tag{A5}$$

Acknowledgments

The work presented here was funded under NASA Subsonic Fixed Wing Hybrid Body Technologies National Research Announcement (NASA NN L08AA02C) with Karen Taminger as the associate principal investigator and Cynthia Lach as the contract officer technical representative. We are thankful to both for their suggestions. The authors would also like to thank our partners in the NRA project, Bob Olliffe and Steve Englestadt, of the Lockheed Martin Aeronautics Company of Marietta, Georgia, for technical discussions. Additionally, the authors would like to thank the members of the Unitized Structure Group. Thanks are also due to Michael Philen for his input into the experimental development. Finally, thanks to the AOE Machine Shop personnel for their expertise and excellent craftsmanship.

References

[1] Smith, S. T., Bradford, M. A., and Oehlers, D. J., "Numerical Convergence of Simple and Orthogonal Polynomials for the Unilateral Plate Buckling Problem Using the Rayleigh–Ritz Method," *International Journal for Numerical Methods in Engineering*, Vol. 44, 1999, pp. 1685–1707. doi:10.1002/(SICI)1097-0207(19990420)44:11<1685::AID-NME562>3.0.CO;2-9

[2] Liew, K. M., Xiang, Y., Kitipornchai, S., and Lim, M. K., "Vibration of Rectangular Mindlin Plates with Intermediate Stiffeners," *Journal of Vibration and Acoustics*, Vol. 116, No. 4, 1994, pp. 529–535. doi:10.1115/1.2930459

[3] Liew, K. M., Xiang, Y., Kitipornchai, S., and Meek, J. L., "Formulation of Mindlin–Engesser Model for Stiffened Plate Vibration," *Computer Methods in Applied Mechanics and Engineering*, Vol. 120, No. 3, 1995, pp. 339–353. doi:10.1016/0045-7825(94)00064-T

[4] Kumar, Y. V. S., and Mukhopadhyay, M., "A New Triangular Stiffened Plate Element for Laminate Analysis," *Composites Science and Technology*, Vol. 60, No. 6, 2000, pp. 935–943. doi:10.1016/S0266-3538(99)00190-6

[5] Bellman, R., Kashef, B. G., and Casti, J., "Differential Quadrature: A Technique for the Rapid Solution of Nonlinear Partial Differential Equations," *Journal of Computational Physics*, Vol. 10, No. 1, 1972, pp. 40–52. doi:10.1016/0021-9991(72)90089-7

[6] Zeng, A., and Bert, C. W., "A Differential Quadrature Analysis of Vibration for Rectangular Stiffened Plates," *Journal of Sound and Vibration*, Vol. 241, No. 2, 2001, pp. 247–252. doi:10.1006/jsvi.2000.3295

[7] Wei, G. W., Zhao, Y. B., and Xiang, Y., "Discrete Singular Convolution and Its Application to the Analysis of Plates with Internal Supports. Part 1: Theory and Algorithm," *International Journal for Numerical Methods in Engineering*, Vol. 55, 2002, pp. 913–946. doi:10.1002/nme.526

[8] Zhao, Y. B., Wei, G. W., and Xiang, Y., "Discrete Singular Convolution for the Prediction of High Frequency Vibration of Plates," *International Journal of Solids and Structures*, Vol. 39, No. 1, 2002, pp. 65–88. doi:10.1016/S0020-7683(01)00183-4

[9] Yeilaghi Tamijani, A., and Kapania, R. K., "Vibration of Plate with Curvilinear Stiffener Using Meshfree Method," AIAA, Paper 2009-2647, May 2009.

[10] Zhou, L., and Zheng, W. X., "Moving Least Square Ritz Method for Vibration Analysis of Plates," *Journal of Sound and Vibration*, Vol. 290, No. 3–5, 2006, pp. 968–990. doi:10.1016/j.jsv.2005.05.004

[11] STAR Modal, Ver. 6.4.0.0, Spectral Dynamics, Inc., San Jose, CA; also http://www.spectraldynamics.com/ [retrieved 19 Oct. 2009].

[12] Martini, L., and Vitaliani, R., "On the Polynomial Convergent Formulation of a C^0 Isoparametric Skew Beam Element," *Computers and Structures*, Vol. 29, No. 3, 1988, pp. 437–449. doi:10.1016/0045-7949(88)90396-3

[13] Kapania, R. K., and Singhvi, S., "Free Vibration Analyses of Generally Laminated Tapered Skew Plates," *Composites Engineering*, Vol. 2, No. 3, 1992, pp. 197–212. doi:10.1016/0961-9526(92)90004-P

[14] Kapania R. K., and Lovejoy, A. E., "Free Vibration of Thick Generally Laminated Cantilever Quadrilateral Plates," *AIAA Journal*, Vol. 34, No. 7, 1996, pp. 1474–1486. doi:10.2514/3.13256

[15] Kapania, R. K., and Kim, Y.-Y., "Flexural-Torsional Coupled Vibration of Slewing Beams Using Various Types of Orthogonal Polynomials," *Journal of Mechanical Science and Technology*, Vol. 20, No. 11, 2006, pp. 1790–1800.

[16] Wessel, J. K., *Handbook of Advanced Materials: Enabling New Designs*, Wiley–Interscience, Hoboken, NJ, 2004.